Exploration Geophysics (2004) ***35****, 137–141*

Apparent Aeromagnetic Wavelengths of the Magnetic Signals of Ocean Swell

F.E.M. (Ted) Lilley[1] Karen A. Weitemeyer[2]

Key Words: aeromagnetic, signals, wavelength, ocean, waves, swell, motional induction

ABSTRACT

Ocean swells have a magnetic signal, caused by the motional induction of seawater moving in the steady main magnetic field of Earth. These signals may be sensed by a low-flying aircraft, carrying out aeromagnetic measurements over the ocean. The apparent spatial wavelength that such signals will have, when observed data are plotted out for geological purposes, can vary greatly. It will depend particularly on the relative speeds and directions of travel of the observing aircraft and the ocean swells. The apparent wavelength of the ocean swell magnetic signal cannot be less than the actual ocean swell wavelength. Generally, it is greater, and it can range up to infinity in value. For observations over continental shelves, the situation is complicated by the dependence of the swell phase-velocity on water depth, by which the swell speed generally slows as land is approached.

INTRODUCTION

A magnetic signal, generated by motional electromagnetic induction, accompanies ocean waves and swell. Seawater moves across the flux-lines of Earth's main magnetic field, and in so doing generates electric currents, which flow through the seawater. These electric currents have their own magnetic fields, which are the magnetic fields generated by the wave motion.

The magnetic fields of ocean waves have been the subject of theoretical investigation by Longuet-Higgins et al. (1954), Weaver (1965), Beal and Weaver (1970), Podney (1975), Chave (1984), and Weaver (1997). Maclure et al. (1964) and Ochadlick (1989) report measurements in agreement with the theory of Weaver (1965), and observations of the magnetic signals of ocean waves are also reported by Fraser (1966) and Watermann and Magunia (1997). In particular, Ochadlick (1989) reports aeromagnetic measurements over deep water.

The topic is naturally closely associated with the electric signals of such waves, which are studied in papers such as Cox et al. (1978) and Hemer et al. (1999). More widely, the topic of electromagnetic induction in the ocean is reviewed by Larsen (1973) and Palshin (1996). Recently, Lilley et al. (2004) observed the magnetic signals of ocean swells with a magnetometer released from a ship to float freely on the surface of the ocean for several days. The signal observed was consistent with knowledge of the swell characteristics at that time, combined with the theory of Weaver (1997).

Low-flying aircraft, engaged in aeromagnetic surveying, may detect the magnetic signals of ocean swell as noise. A first line of defence is simply to fly higher, exploiting the exponential decrease with height that accompanies the swell signal. However, flying higher will also reduce the detail of the geological signal of the crust below the seafloor, which may be the objective of the survey. Thus there will be times when an ocean swell signal is tolerated in the observed data.

The point is made in Lilley et al. (2004) that often the ocean swell signal will be a sharp spectral peak, for a stationary magnetometer. The present paper examines how a moving aircraft sees a different frequency, and how this frequency translates into an apparent spatial wavelength if it is preserved in data that are then plotted in map form. It is seen that the relative speeds and directions of aircraft and ocean swell are critical in determining the apparent spatial wavelength of the ocean swell signal.

INDUCTION THEORY

Motional Induction

Reference is made here to the theory of motional induction of ocean swell as developed by Weaver (1965, 1997). An ocean swell is analysed as a simple harmonic wave on the surface of seawater that is deep in the sense that the depth is much greater than the horizontal wavelength of the wave. The wave propagates in the *x*-direction with wavenumber *m* and angular frequency ω; the phase speed of the wave *c* is thus given by

$$c = \omega / m \tag{1}$$

The magnetic signal $b(x, t)$ in the direction of the main field of Earth (the component measured by a total-field magnetometer) generated by the ocean swell is then given by

$$b(x,t) = b_{\mathrm{F}} \exp i(\omega t - mx) \tag{2}$$

where t denotes time and b_{F}, the amplitude of the magnetic signal of the ocean swell, is given by

$$b_{\mathrm{F}} = \frac{Tag\mu_0\sigma F}{8\pi}\left(\cos^2\theta\cos^2 I + \sin^2 I\right)\exp\left(\frac{-4\pi^2 h}{gT^2}\right) . \tag{3}$$

Here *T* is the period of the wave (sec), *a* is the amplitude (*m*), g is the acceleration due to gravity, μ_0 is the permeability of free space, σ is the electrical conductivity (S/m) of the seawater, *F* is the ambient total magnetic field intensity and *I* the inclination of Earth's main magnetic field, θ is the direction of wave travel measured as an angle positive eastwards from the direction of magnetic north, and *h* is the height (m) of the magnetometer above the sea surface. Introducing a constant *K* given by

$$K = \frac{g\mu_0}{8\pi} \tag{4}$$

[1] *Research School of Earth Sciences, Australian National University*
ACT, Australia 0200
Phone: 02 6125 3406
Fax: 02 6257 2737
Email: ted.lilley@anu.edu.au

[2] *Research School of Earth Sciences, Australian National University*
ACT, Australia 0200
(now at University of California at San Diego, USA)
Email: kweiteme@ucsd.edu

Manuscript Received: July 5, 2003
Revised Version Received: February 19, 2004

a geometric function G(θ, *I*) given by

$$G(\theta,I) = \cos^2\theta\cos^2 I + \sin^2 I \qquad (5)$$

an exponential decay with height A(*h*, *T*) given by

$$A(h,T) = \exp\left(\frac{-4\pi^2 h}{gT^2}\right) \qquad (6)$$

and notation *W* for the amplitude of the total-field magnetic signal per unit amplitude of wave given by

$$W = \frac{b_F}{a} \qquad (7)$$

then *W* may be expressed as

$$W = KTF\sigma\, G(\theta,I)\, A(h,T) \quad . \qquad (8)$$

Note that the value of *W* at the sea-surface (for which $h = 0$ and so A = 1) is linearly proportional to each of the variables *T, F* and σ. The reduction of the signal with height above sea-surface is exponential, and, of the latter three variables, is a function of *T* only. The "1/e folding height" (the height at which the signal is reduced to 1/e of its surface value) is given by $gT^2/4\pi^2$; that is, by g/ω^2 , where ω is the angular frequency of the wave.

Figure 1 demonstrates some characteristics of the function *W* at different latitudes. As latitude increases, *F* generally increases, and σ, which is strongly dependent on temperature, generally decreases. With increasing distance from the equator there is thus a balance of stronger magnetic field against weaker seawater conductivity. At mid-latitudes there is a maximum of the effect, as shown in Figure 1.

For the SWAGGIE area of the Southern Ocean off South Australia (Popkov et al., 2000; Hitchman et al., 2000), for example, representative values for *F*, σ and *I* are 60280 nT, 4.4 S/m and -68.4° respectively. The electrical conductivity is for a surface temperature value of 16°C and a surface salinity of 35.5 (in the "practical" dimensionless units of physical oceanography) taken from maps in Tomczak and Godfrey (1994), combined with tables for the electrical conductivity of seawater in Bullard and Parker (1970). Thus for the sea-surface in the SWAGGIE area (taking g as 9.8 m/s^2)

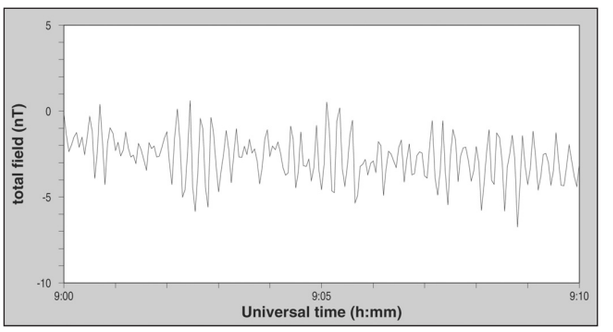

Fig. 2. Observed record from a free-floating magnetometer showing the individual magnetic signals of successive ocean swells, with a typical peak to peak range of 5 nT, from Lilley et al. (2004). Spectral analysis shows the signal to have a sharp spectral peak at 13 s, typical for swells along the south coast of Australia which are generated by storms in the Southern Ocean. According to equation (9), the observed signal indicates a wave height of about 2 m.

$$W = 0.0176\left(\cos^2\theta + 6.38\right)T \quad . \qquad (9)$$

Sea-surface measurements as reported in Lilley et al. (2004) combined with forecast knowledge of the ocean swell at the time confirm that to within the errors involved, actual observed signals are consistent with this theory. An example of the signal from Lilley et al. (2004) is shown in Figure 2. The data in this figure were observed by a floating magnetometer in water depths in the range 2000 to 3000 m, thus satisfying the deep-water requirements of the Weaver theory.

The exponential decrease with altitude for the area will be the general one given for A in equation (6), and shown as a function of wave period in Figure 3. Note that in the altitude range 50 to 200 m (a common height for aeromagnetic surveys) the attenuation of the sea-surface signal is considerable, and sensitive to the period of the swell.

Taking Flight Specifications into Account

Let the ocean swell be travelling at speed *c* in a direction with magnetic bearing *θ*. Let the survey aircraft be travelling at speed

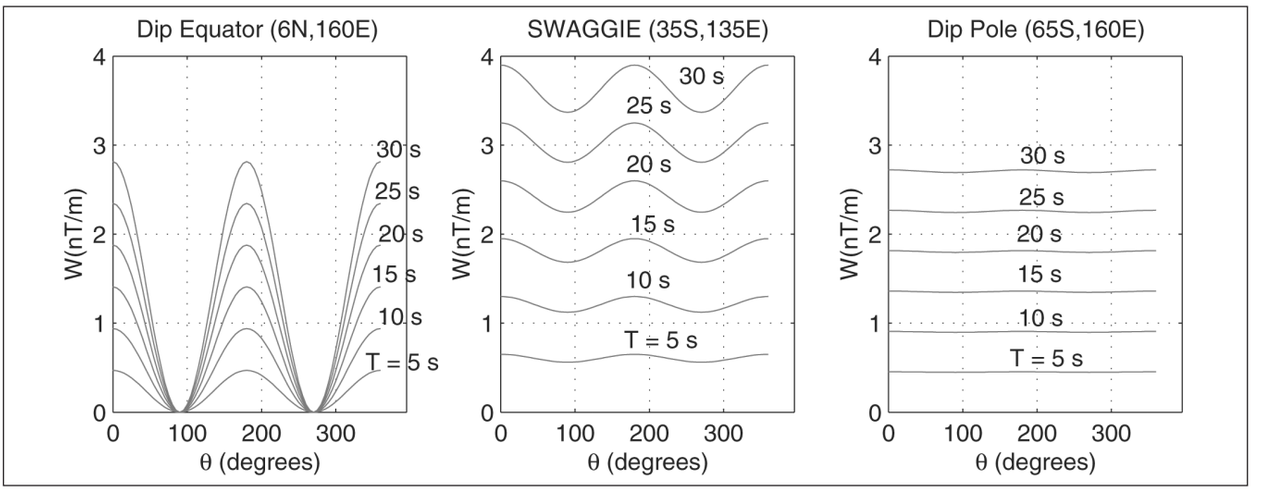

Fig. 1. Sea-surface values of swell magnetic signal (*W*) for different periods of swell, as a function of travel direction of swell (θ, magnetic bearing). Graphs are shown for three different latitudes, ranging from the magnetic dip equator to the magnetic dip pole. These graphs demonstrate the dependence of the signal on both seawater conductivity (σ, which decreases towards the pole) and total magnetic field strength (*F*, which increases towards the pole). The SWAGGIE area is off the Eyre Peninsula of South Australia and is the site of the observations reported by Lilley et al. (2004). The values used in the above graphs for σ and *F* are, respectively, dip equator: 5.0 S/m, 55000 nT; SWAGGIE: 4.4 S/m, 60280 nT; dip pole: 2.8 S/m, 66130 nT.

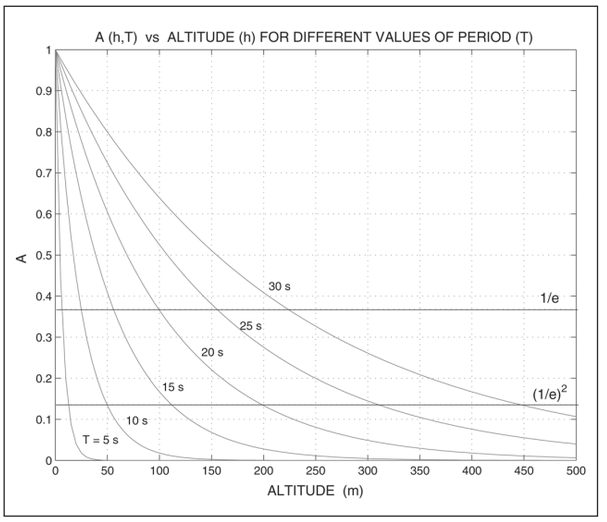

Fig. 3. Exponential decrease of swell signal with height of detector above sea-surface, for different periods of swell.

S in a direction with magnetic bearing ϕ. Denoting the difference (ϕ - θ) by angle α, the speed u of the plane in the direction of wave propagation is given by

$$u = S\cos\alpha \tag{10}$$

and the frequency f' of the swell magnetic signal seen by the plane is given by

$$f' = f - \frac{u}{\lambda} \tag{11}$$

where λ is the wavelength of the ocean swell. When typical values for aircraft and swell speeds are used, this simple equation has important consequences, as will be discussed.

If the observed data are plotted out in map form, the ground wavelength of the swell signal recorded by the aircraft, λ', is

$$\lambda' = \frac{S}{f'} = \frac{S}{f - u/\lambda} \tag{12}$$

and so

$$\lambda' = \frac{S\lambda}{c - u} \quad . \tag{13}$$

The real wavelength λ is thus amplified by a factor $S/(c - u)$, which can be a strong effect as will be shown below. It should be noted that an equation equivalent to equation (11) was used by Ochadlick (1989), following Weaver (1965), when interpreting aeromagnetic observations of swell signals.

DISCUSSION

Some Typical Numerical Values

To aid in their analysis, equations (10), (11), and (13) will now be presented in graph form. In order to give actual numbers to the graphs, a typical value of 60 m/s for aircraft speed will be used. For the swell phase speed a value of 20 m/s will be taken, appropriate for a deep-water swell of typical period 13 s and corresponding wavelength (λ) of 270 m (more accurate values would be 20.8 m/s, 13.3 s and 276 m). Using these values, Figure 4 then shows how the observed frequency (f') and apparent spatial wavelength (λ') of the swell signal varies with the component of

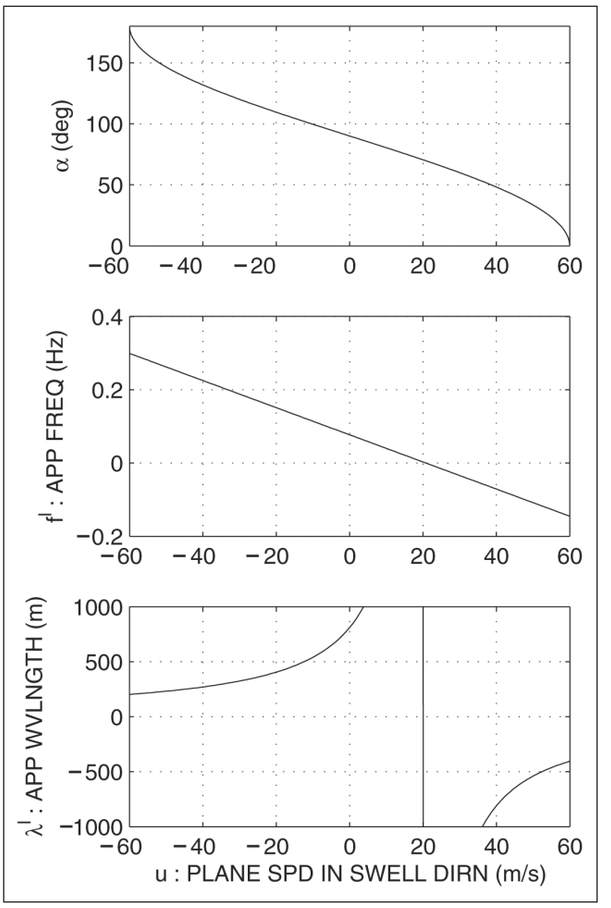

Fig. 4. The top panel shows the relationship expressed in equation (10). The middle and lower panels show the dependence of apparent frequency (f', equation 11) and apparent wavelength (λ', equation 13) respectively on u, the component of plane speed in the direction of swell travel.

the plane speed (u) in the direction of swell travel, according to the theory in the preceding section.

The top panel of Figure 4 illustrates the cosinusoidal behaviour of equation (10), and the middle panel the linear character of equation (11). The lower panel then displays the characteristics of equation (13), with its distinctive asymptote when the plane-speed component u equals the swell speed (at 20 m/s). Negative frequencies and wavelengths occur on the graphs when the plane speed in the direction of the wave travel is greater than the actual wave speed itself. The plane is then "overtaking" the swells, and sees the swells as travelling in the opposite direction to its own travel. Such negative signs do not, however, propagate through into the recorded magnetic data.

This latter graph shows that all wavelengths longer than the actual one (λ) are possible for the apparent wavelength (λ'). The true wavelength (λ) value of 270 m in this case is approached by the apparent wavelength (λ') only for the hypothetical case when plane speed in the direction of the swell travel is much greater than the swell speed. In that (unlikely) case, the relative swell speed is negligible, and the plane is in effect traversing across a swell pattern which it sees as stationary.

Insight is also gained into the phenomenon if f' and λ' are plotted against α, the relative direction of plane and swell. The relevant equations then are equation (10) again together with

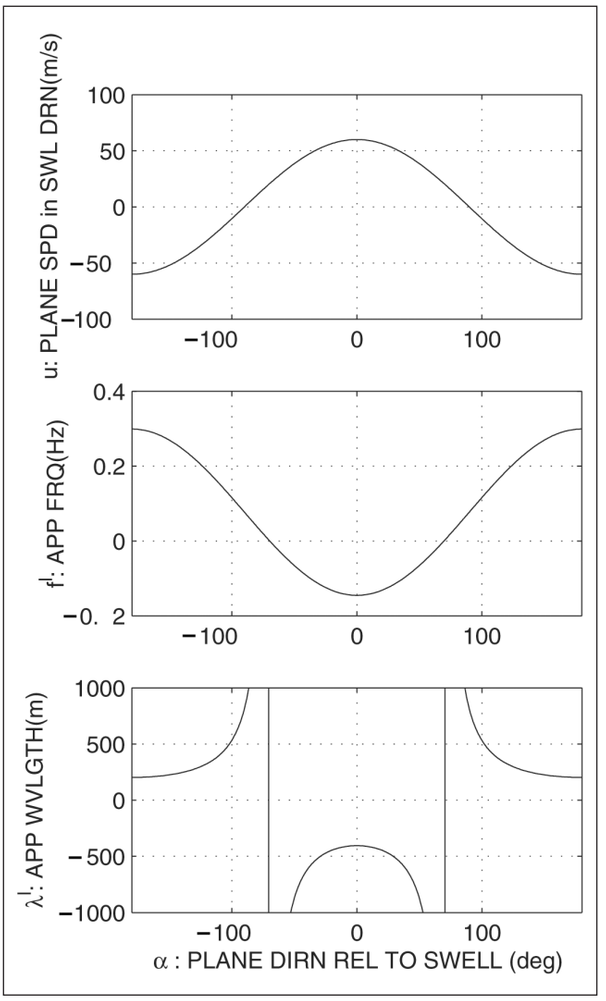

Fig. 5. The top panel shows the relationship expressed in equation (10). The middle and lower panels show the dependence of apparent frequency (f', equation 14) and apparent wavelength (λ', equation 15) respectively on α, the direction of plane travel relative to swell travel.

$$f' = f - \left(\frac{S}{\lambda}\right)\cos\alpha \tag{14}$$

and

$$\lambda' = \frac{S\lambda}{c - S\cos\alpha} \quad . \tag{15}$$

Such graphs are presented in Figure 5. As for Figure 4, particular cases can now be inspected on these graphs. One example is when the component of plane speed in the direction of swell travel is zero: the apparent frequency observed by the plane is then the correct one, but the apparent wavelength is amplified. Another example is when the component of plane speed equals the swell speed: the apparent frequency is then zero, and the apparent wavelength infinite. As can be seen from equation 15, the asymptotes in Figure 5 occur at values of α given by

$$\alpha = \arccos\left(\frac{c}{S}\right) \tag{16}$$

i.e., ± 70.5° in this case.

A graph like the central panel of Figure 5 is presented in Ochadlick (1989), but with the sign of negative frequencies ignored, so that the negative part of the graph is reflected up into the region of positive frequencies.

Some Complications with Ocean Swells on Continental Shelves

The characteristics of ocean swells approaching (Australian) shores at any time are now predicted in both Australian and global models. Australian forecasts may be found at the web site <http://www.bom.gov.au>, and global forecasts at the web site <http://www.ncep.noaa.gov>. The characteristics predicted are period, amplitude, and direction of propagation of the ocean swells.

However, what happens as the swell comes in across a continental shelf is not usually evident in such models, which are on too coarse a scale. Further, the situation may be expected to become complicated by the swell changing from a "short" or deep-water wave over deep ocean, to a "long" or shallow-water wave over the continental shelf, as a result of its wavelength (typically several hundred metres) becoming greater than the water depth.

Texts of physical oceanography such as Pond and Pickard (1983, page 212) point out that for "short" ocean waves and swell, where the ocean depth is greater than the wavelength, the phase speed c_s of an ideal swell is given by

$$c_S = \left(g/m\right)^{1/2} \tag{17}$$

whereas in shallow water, where the ocean depth (z) is less than the wavelength, an ideal swell is a "long" wave, with phase speed c_L given by

$$c_L = \left(g\,z\right)^{1/2} \quad . \tag{18}$$

An important contrast between equations (17) and (18) is the independence of the former on ocean depth, while the latter has an ocean-depth dependence. Thus ocean swells, of typical wavelength several hundred metres, are short waves over deep ocean but long waves over continental shelves, especially as they approach shore. Coming across the continental slope they will be in a transition mode between short and long wavelength behaviour.

Long-wave behaviour thus involves a phase speed that is a function of ocean depth. As can be seen from equation (18) phase speed reduces as water shallows, a general consequence of a swell approaching shore. This change in speed also has a further complication in that refraction effects may lead to a change in the travel direction of the swell. If the travel direction is oblique to the coast, it may be brought around to head directly to shore. An associated effect is that as the swell approaches the shore in shallowing water its energy is dissipated, and its magnetic signal reduced.

Aeromagnetic surveys are more likely to be over continental shelves, and across the shore line onto land, than over deep sea. The complication of swell propagation on continental shelves suggests further study of magnetic signal generation is required, both theoretical and observational, for a complete understanding of the phenomenon.

While complicated by the slowing of a swell as water shallows, inspection of Figure 4 and Figure 5 does however suggest a strategy which might offer at least a partial solution to the swell signal problem: the choosing of an aircraft flight direction such that λ' is very large, and the signal of perhaps several nT is distributed along several km of flight path. Evidently, this effect may be achieved if the component of the aircraft speed in the

direction of the swell is close to the speed of travel of the swell. In Figure 4, a value of u which is within 15 m/s of the swell speed will distribute the signal of each swell over more than 1000 m. In Figure 5, the equivalent is achieved by a flight direction within 15° of those for which the asymptotes occur (± 70.5°).

Typical Aeromagnetic Survey Flight Patterns

In the interests of efficiency, aeromagnetic survey planes commonly fly alternate lines in opposite directions. That is, having completed a line in one direction, the aircraft turns around, adjusts its position laterally by some distance (the line spacing), and heads back in the direction from which it has just come.

Choosing an optimum direction for flight lines then becomes the task of choosing a direction which is optimum both for lines flown in that direction, and in that direction reversed. In terms of angle α in Figure 5, the two directions of α and ($\alpha \pm 180°$) should be considered together.

Such an extra factor, of lines flown in the reverse direction, may strongly affect the choice of direction for lines flown in the forward direction. However, a suitable choice of α which distributes swell signal along an extended apparent wavelength may still be possible. From Figure 5 it is clear that a basic choice is

$$\alpha = 90° \qquad (19)$$

which is the case where flight-line direction is perpendicular to swell direction. Then, in Figure 5, there is a symmetry for the two α values of 90° and -90°, and the apparent wavelength values (λ') will be the same for each: 810 m in this particular example (using equation 15).

CONCLUSIONS

Swell magnetic signals are within the measurement capability of aeromagnetic survey aircraft. Careful attention to relative speed and direction must be made if the swell signals are to be adequately removed from observed data.

Forecasts are now available for the swell to be expected along Australia's southern coast, the origin of which is largely storms in the Southern Ocean. Using the appropriate theory, the magnetic swell signal to be expected at any time can also be forecast. If aircraft speed over the ground is known accurately, the apparent frequency of the swell signal as observed by the aircraft, f', may be predicted. This estimate may provide a useful guide to filtering the signal from observed data.

Under some circumstances, a helpful strategy may be to direct the aircraft so that the component of its speed in the direction of swell travel is close to the speed of the swell. The situation is however complicated by the dependence of swell speed on water depth, as swells travel across a continental shelf. Also practical matters, such as survey patterns in which lines are flown in opposite directions, may suggest flying lines at right angles to the direction of swell propagation.

The present work has focused on how known aircraft speed and direction can be used to quantitatively map the apparent frequency and wavelength of the magnetic signal of deep-ocean swell. The analysis lays the foundation for further research into the topic, to account for more complicated variations in swell speed and direction as ocean swells travel across a continental shelf into shallower coastal waters, which serve as likely areas for marine magnetic surveys.

ACKNOWLEDGEMENTS

We thank Peter Milligan for valuable discussion. Karen Weitemeyer acknowledges summer research scholarship support at the Research School of Earth Sciences, Australian National University, in early 2003. We thank Stefan Maus, Julian Vrbancich, and Lindsay Thomas for valuable suggestions that led to improvements in the manuscript.

REFERENCES

Beal, H.T. and Weaver, J.T., 1970, Calculations of magnetic variations induced by internal ocean waves: *Journal of Geophysical Research*, **75**, 6846–6852.

Bullard, E.C. and Parker, R.L., 1970, Electromagnetic induction in the oceans: in Maxwell, A.E. (ed.), *The Sea*: Wiley-Interscience, **4**, 695–730.

Chave, A.D., 1984, On the electromagnetic fields induced by oceanic internal waves: *Journal of Geophysical Research*, **89**, 10519–10528.

Cox, C.S., Kroll, N., Pistek, P. and Watson, K., 1978, Electromagnetic fluctuations induced by wind waves on the deep sea floor: *Journal of Geophysical Research*, **83**, 431–442

Fraser, D.C., 1966, The magnetic fields of ocean swell: *Geophysical Journal of the Royal Astronomical Society*, **11**, 507–517.

Hemer, M.A., Heinson, G.S., Bye, J.A.T. and White, A., 1999, Wave energy turbulence spectra from the measurement of electric fields in the ocean: in Banner, M.L. (ed.), *The wind-driven air-sea interface*: University of New South Wales, Sydney, 49–56.

Hitchman, A.P., Lilley, F.E.M. and Milligan, P.R., 2000, Induction arrows from offshore floating magnetometers using land reference data: *Geophysical Journal International*, **140**, 442–452.

Larsen J.C., 1973, An introduction to electromagnetic induction in the ocean: *Physics of the Earth and Planetary Interiors*, **7**, 389–398.

Lilley, F.E.M., Hitchman, A.P., Milligan, P.R. and Pedersen, T., 2004, Sea-surface observations of the magnetic signals of ocean swells: *Geophysical Journal International*, in press.

Longuet-Higgins, M.S., Stern, M.E. and Stommel, H., 1954, The electric field induced by ocean currents and waves, with applications to the method of towed electrodes: *Papers in Physical Oceanography and Meteorology*, **13**, 1–37.

Maclure, K.C., Hafer, R.A. and Weaver, J.T. 1964, Magnetic variations produced by ocean swell: *Nature*, **204**, 1290–1291.

Ochadlick, A.R., 1989, Measurements of the magnetic fluctuations associated with ocean swell compared with Weaver's theory: *Journal of Geophysical Research*, **94**, 16237–16242.

Palshin, N.A., 1996, Oceanic electromagnetic studies: a review: *Surveys of Geophysics*, **17**, 455–491.

Podney, W., 1975, Electromagnetic fields generated by ocean waves: *Journal of Geophysical Research*, **80**, 2977–2990.

Pond, S. and Pickard, G., 1983, *Introductory dynamical oceanography, 2nd edition*: Pergamon Press.

Popkov, I., White, A., Heinson, G., Constable, S., Milligan, P. and Lilley, F.E.M., 2000, Electromagnetic investigation of the Eyre Peninsula conductivity anomaly: *Exploration Geophysics*, **31**, 187–191.

Tomczak, M. and Godfrey, J.S., 1994, *Regional oceanography: an introduction*: Pergamon Press.

Watermann, J. and Magunia, A., 1997, Propagation parameters of sea surface waves inferred from observations from two closely spaced vector magnetometers: *Journal of Geomagnetism and Geoelectricity*, **49**, 709–720.

Weaver, J.T., 1965, Magnetic variations associated with ocean waves and swell: *Journal of Geophysical Research*, **70**, 1921–1929.

Weaver, J.T., 1997, Generation of magnetic signals by waves and swell: in Milligan, P.R. and Barton, C.E. (eds.), *Transient and induced variations in aeromagnetics*: Australian Geological Survey Organisation Record 1997/27, 15–16.